Hindawi Publishing Corporation
International Journal of Microwave Science and Technology
Volume 2012, Article ID 791635, 7 pages
doi:10.1155/2012/791635

Research Article

A Systemic Approach to the Compensation of Rain Attenuation in Ka-Band Communication Satellites

Piero Angeletti[1] and Marco Lisi[2]

[1] *Directorate of Technical & Quality Management, European Space Agency, Keplerlaan 1, 2200 AG Noordwijk, The Netherlands*
[2] *Directorate of Galileo Programme & Navigation Related Activities, European Space Agency, Keplerlaan 1, 2200 AG Noordwijk, The Netherlands*

Correspondence should be addressed to Marco Lisi, marco.lisi@esa.int

Received 4 March 2012; Revised 14 September 2012; Accepted 14 September 2012

Academic Editor: Borja Vidal

Rain attenuation at Ka-band is a severe phenomenon that drastically impairs satellite communications at these frequencies. Several adaptive compensation techniques have been elaborated to counteract its effects and most often applied one at a time. The present paper proposes the contemporary exploitation of different techniques in a combined approach. Such an integrated approach is thoroughly analyzed in a simplified scenario and will be shown to achieve a very effective solution, making the Ka-band spectrum fully available for broadband satellite applications and network-centric systems.

1. Introduction

The advent of Ka-band (The frequency bands 17.7–21.2 GHz (space to Earth) and 27.5–31 GHz (Earth to space) have been allocated by the International Telecommunication Union (ITU) for the use of Fixed Satellite Services (FSS)) satellite communications is driven by the diffusion of consumer applications (such as High Definition Television broadcasting) and by the increased demand for broadband networks in network-centric systems.

The network-centric architecture, originally conceived for military applications, is becoming a paradigm for large integrated systems, or "systems of systems", able to collect and to convey data seamlessly throughout a number of different possible media and to deliver useful information after a data fusion process.

Ka-band space segment and ground segment technologies, after a pioneering phase (Italsat [1, 2], ACTS [3]) and a successive consolidation, are now mature for cost-effective and reliable commercial missions.

One the major drawbacks still affecting Ka-band satellite communications is that related to rain attenuation.

Rain attenuation in satellite communication systems operating at Ka-band frequencies is much more severe than that usually experienced at lower frequency bands: rain attenuation at 20 GHz (Ka-band down-link), for instance, is almost three times that at 11 GHz (Ku-band down-link) [4, page 125]. This fact makes rain attenuation one of the most important limiting factors to be taken into account in the design of a 20/30 GHz satellite communication system.

A number of mitigation techniques has been envisioned and experimented over the years, in the attempt to overcome the problem and to make Ka-band satellite applications as commercially viable as those at Ku band [5, Chapter 8].

One first classification of such techniques is between ground-based and space-based solutions.

Ground-based techniques are those basically operated on ground (either in open- or closed-loop configurations) and only indirectly affecting the satellite payload. Among them are Up-Link Power Control (both for transparent and regenerative payloads), End-to-End Power Control (for transparent payloads only), Adaptive Coding and/or Modulation, Site Diversity, and Terrestrial Back-Ups.

Space-based techniques involve, in one way or another, an adaptive use of the payload resources to counteract rain attenuation.

Down-Link Power Control is a technique suitable for both "bent pipe" and regenerative payloads. Adaptive Coding

and Adaptive Modulation techniques can be used, in regenerative payload, to adapt the down-link signal characteristics to rain attenuation, independently from the up-link signal.

Adaptive down-link antennas allow a reconfiguration of the gain distribution over the coverage to compensate for higher rain attenuations in specific areas. Contoured beam antennas (in array-fed reflector configurations) can achieve such capability by incorporating variable components (such as variable power dividers) into their beam forming networks.

Active phased-array antennas (either in "array-fed reflector" or in "direct radiating array" configurations) offer an even better control of the down-link EIRP. In an active down-link antenna each radiating element (feed or subarray) is individually fed by a transmit active module (solid-state power amplifier). These antennas not only allow a fast and effective reconfiguration of the gain distribution over the coverage, but also make possible, in case of multiple-beam configurations, a full reallocation of the RF power among the radiated beams. In an active phased-array antenna all active modules (power amplifiers in this case) contribute to the formation of any single beam; this implies that the overall RF power can be dynamically shared among the beams (Power Reconfigurability). On the opposite end, in conventional focused reflector antennas each feed (and its corresponding power amplifier) is virtually associated to only one beam, hence traffic reconfigurability is impossible.

An alternative adaptive antenna configuration is the Multibeam Adaptive Antenna (MAA) concept, which allows a flexible sharing of the total power from the power amplifier modules among the beams by means of a Multiport Power Amplifier (MPA). The application of this antenna configuration to counteract rain attenuation at Ka band was proposed for future generations of Italsat satellites as early as in 1989 [6, 7], and it is still subject of intense R and D [8–11]. While the above summarized adaptive compensation techniques are most often applied one at the time, the development of the technology and the highly integrated nature of today's satellite communication systems suggest combined approaches, implementing several techniques in parallel in a dynamic configuration.

In particular in the following paragraphs we will focus our attention on the downlink of a multibeam Ka-band system. After a general discussion about individual and joint benefits of Adaptive Coding and Modulation (ACM) and Down-Link Power Control, the proposed integrated approach will be thoroughly analyzed in a simplified scenario.

2. Overview of Adaptive Coding and Modulation Techniques

Adaptive Coding and Modulation (ACM) techniques, applied in interactive and point-to-point applications, provide efficient dynamic link adaptation to propagation conditions, targeting each individual earth station.

The adaptation is obtained by varying the air interface characteristics in terms of modulation constellation and coding scheme. The aim is to allow each user to have a modulation and coding such that at the considered BER the associated required Signal-to-Noise-plus-Interference Ratio (SNIR) is compatible with the experienced atmospheric losses and cochannel interference. It is worth noting that for its efficacy ACM has been selected as baseline for the next generation of the Digital Video Broadcasting via Satellite standard (DVB-S2) [12].

Link adaptation is achieved informing the satellite up-link station of the channel condition (i.e., SNIR) of each earth station via the satellite return link. Each link operates dynamically exploiting the SNIR to the maximum spectral efficiency. The set of standardized DVB-S2 modes (combination of symbol constellation and coding rates) hinges on the revitalized use of Low Density Parity Check (LDPC) error correction codes initially introduced by Gallager in the 60's [13].

The net result is the availability of a fine granularity in the Spectral Efficiency versus SNIR curve (refer to Figure 1), resembling the Shannon's bound,

$$\frac{R_b}{B} \leq \log_2\left(1 + \frac{E_S}{N_0 + I_0}\right) \text{[bits/Hz]}, \tag{1}$$

where R_s is the symbol rate, B is the bandwidth, and $E_S/(N_0 + I_0)$ is the SNIR in terms of symbol energy E_s, noise spectral density N_0, and interference spectral density density I_0.

Satellite throughput gains of ACM systems have been estimated to reach a capacity increase up to 100%–200% with respect to constant coding and modulation systems (e.g., DVB-S) [12]. In addition, service availability can be extended.

3. An Integrated Approach

Adaptive coding and modulation techniques allow to effectively comply with different link conditions providing to the users the maximum data-rate permitted with the experienced Signal-to-Noise-plus-Interference Ratio (SNIR). This approach maximizes the individual link exploitation (in terms of spectral efficiency) and the overall system capacity evaluated as sum over all the coverage of active users spectral efficiencies. The availability of a large number of coding and modulation combinations allows to close the link budget in severe interference and fading conditions. The result is an increased link availability at low data rates and a high overall system capacity on a best-effort base. When minimum guaranteed data-rates with certain availabilities are required, the system dimensioning must still rely on power margins on the worst case link budget condition. These power margins, later on, can be fully exploited at operational level to increase the overall capacity on a best effort base.

On the other hand, adaptive power allocation techniques aim at reducing individual power margins by means of an adaptive redistribution of the available RF power based on the real-time needs. The achievement of this objective is strictly dependent on the architecture of the payload high-power section. The idea is to have a common power pool from which a channel can adaptively draw the power it requires. Two candidate solutions are nowadays debated.

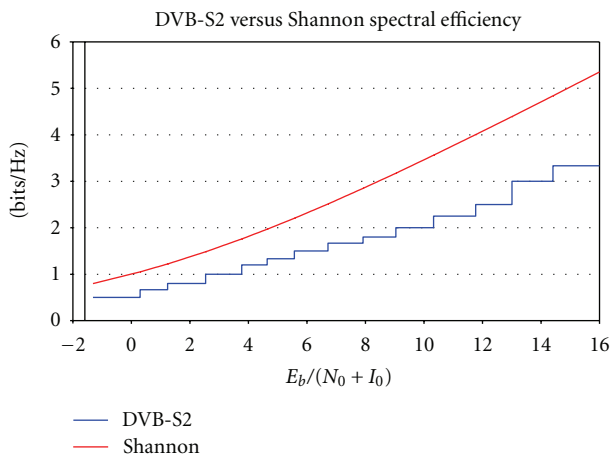

Figure 1: Spectral efficiency—DVB-S2 versus Shannon's bound.

(i) Flex TWTAs: the power pool is realized at the level of the satellite platform DC power capacity. Each individual TWTA can arbitrarily change (within a range that in current developments is about 3-4 dBs) its saturated RF output power while maintaining a constant efficiency (hence, a DC power consumption proportional to the RF output power) [14]. In nominal conditions, the TWTAs are operated at their minimum saturated RF output power, while the DC power subsystem is over dimensioned, in order to have headroom in case of rain fading. It is worth noting that a Flex TWTA does not allow a fast variation of its bias conditions.

(ii) Multiport amplifiers: the power pool is realized at RF power level. The sharing flexibility is achieved through the parallel amplification of all signals by a stack of Power Amplifiers [15–22].

A joint Adaptive Coding and Modulation (ACM) and Down-Link Power-Control approach can be proven to be advantageous in case a minimum data-rate and an associated availability are required and can be traded off with the overall best-effort system capacity. The approach consists in operating the payload in an RF power-pooled configuration [1, 2, 9], so that faded beams can be adaptively boosted to counteract rain attenuation. The system can be optimized to redistribute the power among beams in fading and clear sky conditions, guaranteeing the achievement of all the required data rates and of the availability performance.

To better understand the close relationship between the rain countermeasure on a faded earth station and the remaining population in clear sky we developed a simplified two-cochannel beams model that is reported in the following subparagraphs.

3.1. Rain Attenuation Impairments on the Signal-to-Noise Ratio. The receiver system temperature can be evaluated as:

$$T_S = T_A + \left(L_{\text{preRX}} - 1\right) \cdot T_{\text{Amb}} + L_{\text{preRX}}\ T_{\text{eqRX}}, \tag{2}$$

where T_A is the antenna temperature, L_{preRX} is the passive section loss (from the antenna to the receiver), T_{Amb} is the ambient temperature (working temperature of the passive section), and T_{eqRX} is the effective input noise temperature of the receiver. In clear sky, the antenna temperature (apex C) can be decomposed in sky ($T_{A,\text{Sky}}$) and the ground ($T_{A,\text{Gnd}}$) temperatures as seen by the antenna:

$$T_A^C = T_{A,\text{Sky}} + T_{A,\text{Gnd}}, \tag{3}$$

while in rain conditions (apex R), the antenna temperature (T_A^R) becomes:

$$T_A^R = \frac{T_{A,\text{Sky}}}{L_R} + \left(\frac{L_R - 1}{L_R}\right) T_R + T_{A,\text{Gnd}}, \tag{4}$$

where T_R is the rain temperature, and L_R is the rain attenuation. In summary we can write:

$$T_S^C = T_{A,\text{Sky}} + T_{A,\text{Gnd}} + \left(L_{\text{preRX}} - 1\right) \cdot T_{\text{Amb}} + L_{\text{preRX}} T_{\text{eqRX}}, \tag{5}$$

$$\begin{aligned} T_S^R &= \frac{T_{A,\text{Sky}}}{L_R} + \left(\frac{L_R - 1}{L_R}\right) T_R + T_{A,\text{Gnd}} \\ &\quad + \left(L_{\text{preRX}} - 1\right) \cdot T_{\text{Amb}} + L_{\text{preRX}} T_{\text{eqRX}} \\ &= T_S^C \left[1 + \left(\frac{L_R - 1}{L_R}\right)\left(\frac{T_R - T_{A,\text{Sky}}}{T_S^C}\right)\right]. \end{aligned} \tag{6}$$

The closure of the link budget requires a minimum Signal-to-Noise value that in the following we will consider in terms of symbol energy over noise spectral density:

$$\left(\frac{E_s}{N_0}\right) \geq \left(\frac{E_s}{N_0}\right)_{\text{req}} \equiv \rho_{\text{req}}. \tag{7}$$

In clear sky conditions we can explicit E_s^C in terms of the satellite transmitted power in the beam/channel (P^{Sat}), the satellite antenna gain (G^{Sat}), the free space loss (L), and the Earth Station antenna gain (G_{ES}):

$$E_s^C = \frac{1}{R_s} \cdot \frac{G^{\text{Sat}} P^{\text{Sat}}}{L} \cdot G_{\text{ES}} \tag{8}$$

and for the noise spectral density, K being the Boltzman constant:

$$N_0^C = K T_S^C. \tag{9}$$

In summary, in clear sky we have

$$\left(\frac{E_s}{N_0}\right)^C = \frac{G^{\text{Sat}} P^{\text{Sat}}}{R_s L G_{\text{ES}} K T_S^C}. \tag{10}$$

Similarly, substituting L with LL_R and introducing (6) in (10), we can explicit this ratio in rain conditions:

$$\left(\frac{E_s}{N_0}\right)^R = \left[L_R + (L_R - 1)\left(\frac{T_R - T_{A,\text{Sky}}}{T_S^C}\right)\right]^{-1} \left(\frac{E_s}{N_0}\right)^C. \tag{11}$$

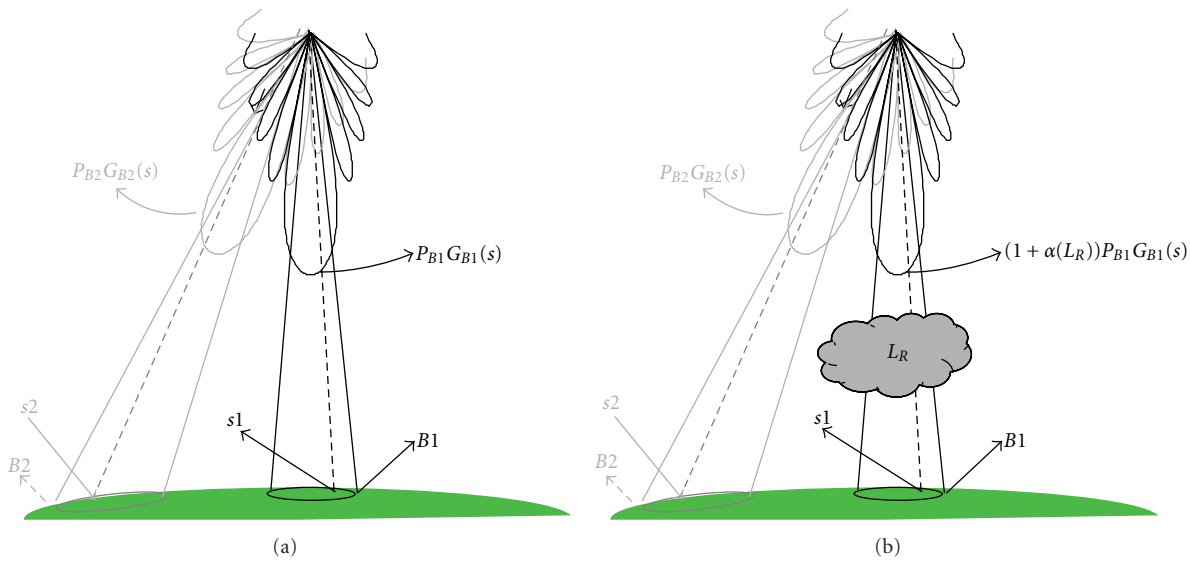

Figure 2: Multibeam antenna geometry ((a) clear sky, (b) fading in Beam-1).

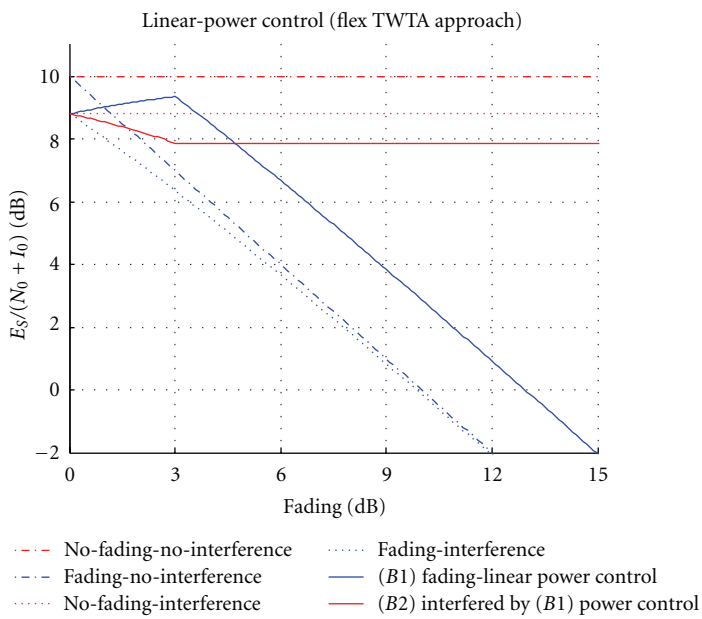

Figure 3: Bidimensional link budget analysis (flex TWTAs with linear power control).

3.2. Rain Attenuation Impairments on the Signal-to-Noise-Plus-Interference Ratio. In a multibeam system with frequency reuse, several beams make use of the same frequency causing cochannel interference that must be duly considered in the link closure condition (7), that becomes:

$$\left(\frac{E_s}{N_0+I_0}\right) \geq \left(\frac{E_S}{N_0+I_0}\right)_{\text{req}} \equiv \rho_{\text{req}}. \tag{12}$$

A pictorial representation of a two cochannel beams system is shown in Figure 2. The two beams are indicated as Beam-1 ($B1$) and Beam-2 ($B2$); $s1$ and $s2$ refer to two ground stations served by Beam-1 and Beam-2, respectively. The statistical independence of thermal noise (N_0) and cochannel interference (I_0) allows the separation of the two different contributions:

$$\begin{aligned}\left(\frac{E_s}{N_0+I_0}\right) &= \left(\left(\frac{E_s}{N_0}\right)^{-1}+\left(\frac{E_s}{I_0}\right)^{-1}\right)^{-1}\\ &= \left(\left(\frac{N_0}{E_s}\right)+\left(\frac{I_0}{E_s}\right)\right)^{-1}.\end{aligned} \tag{13}$$

A link equation can be written for each user/beam. In clear sky conditions we have (14) (reversing symbol energy and noise/interference eases the understanding of the complex coupled behavior); while in case of rain fading over $s1$ in Beam-1 we can write (15).

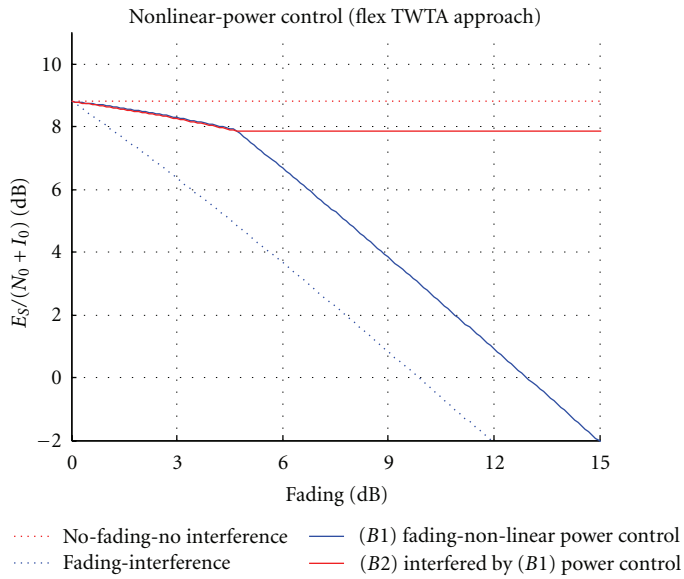

Figure 4: Bidimensional link budget analysis (flex TWTAs with nonlinear power control).

To counteract the fading of $s1$ in Beam-1, the satellite can increase the power of Beam-1 as a generic function of the rain attenuation ($\alpha(L_R)$). Two possible strategies can be foreseen based on the different high-power sections described above.

3.2.1. Power Control with Flex TWTAs. The faded beam output power is increased without changing the power level of the other beams. This can be implemented, for example, increasing the saturation power of a flex TWTA; however, the maximum delta-power is limited by the tube technology. The power increase has two beneficial effects on the faded beam: a compensation of the rain losses and an advantage in terms of Signal-to-Interference. However, an increase of the interference is experienced by the other beams, (refer to (16) for the two-beam model).

3.2.2. Power Control with Multiport Amplifiers. The overall RF power constitutes a unique pool. An increase of the power dedicated to one beam of an amount equal to $\alpha(L_R)$ means an equivalent decrease of the power available to the other beams. In this case the delta-power could reach the overall RF Power-Pool amount (e.g., the sum of the power of all the TWTAs constituting an MPA). The reduction in interfering power sums up to the already referred beneficial effects on the faded beam. On the other hand, nonfaded beams suffer, together with a higher interference level, a decreased power. The simplified equation for a two-beam system is (17).

A fair comparison between the two power control approaches with and without power-pooling must take into account that both systems should be dimensioned for the same maximum RF power (or DC power). In this case the power-pooling approach can benefit from a higher clear-sky operating point, equal to the total available RF power divided by the number of active channels/beams (this advantage has been considered in the following graphs).

Clear Sky. Consider

$$\begin{aligned}\left(\frac{N_0+I_0}{E_s}\right)^C_{(s1)} &= \left(\frac{N_0}{E_s}\right)^C_{(s1)} + \left(\frac{I_0}{E_s}\right)^C_{(s1)},\\ \left(\frac{N_0+I_0}{E_s}\right)^C_{(s2)} &= \left(\frac{N_0}{E_s}\right)^C_{(s2)} + \left(\frac{I_0}{E_s}\right)^C_{(s2)}.\end{aligned} \tag{14}$$

Rain Fading over Beam-1. Consider

$$\begin{aligned}\left(\frac{N_0+I_0}{E_s}\right)^R_{(s1)} &= \left[L_R + (L_R-1)\left(\frac{T_R - T_{A,\mathrm{Sky}}}{T_S^C}\right)\right]\\ &\quad\times \left(\frac{N_0}{E_s}\right)^C_{(s1)} + \left(\frac{I_0}{E_s}\right)^C_{(s1)},\\ \left(\frac{N_0+I_0}{E_s}\right)^R_{(s2)} &= \left(\frac{N_0}{E_s}\right)^C_{(s2)} + \left(\frac{I_0}{E_s}\right)^C_{(s2)}.\end{aligned} \tag{15}$$

Rain Fading over Beam-1, Power Control with Flex TWTAs. Consider

$$\begin{aligned}\left(\frac{N_0+I_0}{E_s}\right)^R_{(s1)} &= \frac{1}{1+\alpha(L_R)}\left[L_R + (L_R-1)\left(\frac{T_R - T_{A,\mathrm{Sky}}}{T_S^C}\right)\right]\\ &\quad\times \left(\frac{N_0}{E_s}\right)^C_{(s1)} + \frac{1}{1+\alpha(L_R)}\left(\frac{I_0}{E_s}\right)^C_{(s1)},\\ \left(\frac{N_0+I_0}{E_s}\right)^R_{(s2)} &= \left(\frac{N_0}{E_s}\right)^C_{(s2)} + [1+\alpha(L_R)]\left(\frac{I_0}{E_s}\right)^C_{(s2)}.\end{aligned} \tag{16}$$

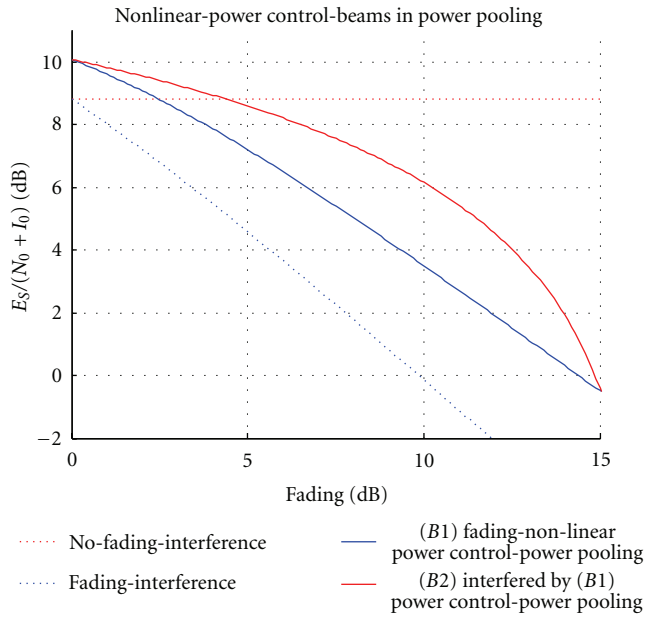

Figure 5: Bidimensional link budget analysis (multiport amplifier with nonlinear power control).

Rain Fading over Beam-1, Power Control with Multiport Amplifiers. Consider

$$\left(\frac{N_0+I_0}{E_s}\right)^R_{(s1)} = \frac{1}{1+\alpha(L_R)}\left[L_R + (L_R-1)\left(\frac{T_R - T_{A,\text{Sky}}}{T_S^C}\right)\right] \times \left(\frac{N_0}{E_s}\right)^C_{(s1)} + \frac{1-\alpha(L_R)}{1+\alpha(L_R)}\left(\frac{I_0}{E_s}\right)^C_{(s1)},$$

$$\left(\frac{N_0+I_0}{E_s}\right)^R_{(s2)} = \frac{1}{1-\alpha(L_R)}\left(\frac{N_0}{E_s}\right)^C_{(s2)} + \frac{1+\alpha(L_R)}{1-\alpha(L_R)}\left(\frac{I_0}{E_s}\right)^C_{(s2)}. \tag{17}$$

3.3. Results. Results of the performed analysis are reported in the figures. SNR/SNIR referring to the faded beam are represented in blue, those referring to the clear-sky beam in red.

Examining Figure 3, dot-dash curves refer to an interference-free case: the faded beam SNR degrades linearly with rain attenuation while the clear-sky SNR stays constant (10 dB). Dot curves account for interference (15 dB in the examples) and no power control. Solid curves refer to power compensation proportional to the rain attenuation without power-pooling; it is clear that the overshooting of the blue curve is due to the advantage in Signal-to-Interference Ratio (SIR) that the faded beam gains with respect to the noncompensated beam. Once the maximum TWTA power is reached (twice the nominal level, in the example) further compensation is not possible and the decay follows the attenuation.

Figure 4 shows a similar analysis (power compensation with Flex TWTAs) with the compensation law optimized to maintain the system performance constant all over the coverage up to the maximum compensation range of a single TWTA (3 dB assumed as in Figure 3).

Finally, Figure 5 shows that the power pooling architecture based on multiport amplifiers (or active antennas as DRAs) with an optimized compensation law outperforms all the previous results in terms of achievable compensation depth (better SNIR at maximum attenuation depth), still maintaining a high overall capacity.

4. Conclusions

The present paper proposed and analyzed the contemporary exploitation of different rain fading countermeasures in a combined approach, based on advanced payload architectures exploiting power-pooling capabilities. Such an integrated approach is thoroughly analyzed in a simplified scenario and it is shown to achieve a very effective solution for the minimum data-rate/availability requirement; at the same time, it preserves the ACM characteristic feature of offering increased capacity on a best-effort basis. The proposed approach makes the Ka-band spectrum fully available for broadband satellite applications and network-centric systems.

References

[1] F. Marconicchio and A. Rodotà, "The ITALSAT program," *Rivista Tecnica Selenia*, vol. 2, no. 4, pp. 21–26, 1990.

[2] A. Paraboni, G. Masini, M. Mauri, R. Polonio, and C. Riva, "Summary of propagation results obtained in 5 years of ITALSAT experiment in Milano," *International Journal of Satellite Communications*, vol. 17, no. 2-3, pp. 169–175, 1999.

[3] R. T. Gedney, R. Schertler, and F. Gargione, *The Advanced Communications Technology Satellite*, SciTech Publishing, 2001.

[4] B. R. Elbert, *Introduction to Satellite Communication*, Artech House, 3rd edition, 2008.

[5] L. J. Ippolito, *Satellite Communications Systems Engineering*, John Wiley & Sons, 2008.

[6] M. Lisi and G. Perrotta, "An integrated 20/30 GHz multibeam/multiport antenna system for fixed satellite services," in *Proceedings of the ISAP*, Tokyo, Japan, 1989.

[7] M. Lisi and G. Panariello, "An adaptive multibeam antenna for italsat future generation satellites," in *Proceedings of the 15th AIAA International Communications Satellite Systems Conference (ICSSC '94)*, San Diego, Calif, USA, 1994.

[8] A. Paraboni, P. Gabellini, A. Martellucci, P. Rinous, C. Capsoni, and N. Gatti, "Proposed architectures for a reconfigurable Ka-Band antenna front-end for active rain fade compensation," in *Proceedings of the 28th ESA Antenna Workshop*, Noordwijk, The Netherlands, 2005.

[9] A. Paraboni, C. Capsoni, M. Buti et al., "Assessment of performance of a ka-band broadcasting reconfigurable satellite antenna with adaptive mitigation for atmospheric attenuation," in *Proceedings of the European Conference on Antennas and Propagation (EuCAP '06)*, Nice, France, November 2006.

[10] P. Angeletti, A. Bolea-Alamañac, M. Bousquet, and M. Lisi, "Joint exploitation of interference and fading mitigation techniques inmultibeam power-pooling satellite systems," in *Proceedings of the 25th AIAA International Communications Satellite Systems Conference*, Seoul, Korea, April 2007.

[11] P. Gabellini, C. Capsoni, A. Martellucci, N. Gatti, L. Resteghini, and P. Rinous, "A reconfigurable multi-matrix antenna front-end architecture for Ka-Band broadcasting satellite services," in *Proceedings of the 2nd ESA Workshop on Advanced Flexible Telecom Payloads*, Noordwijk, The Netherlands, April 2012.

[12] ETSI EN 302 307, Digital Video Broadcasting, "Second Generation framing structure, channel coding and modulation systems for Broadcasting, Interactive Services, News Gathering and other broadband satellite applications".

[13] R. G. Gallager, "Low density parity check codes," *IEEE Transactions on Information Theory*, vol. 8, no. 1, pp. 21–28, 1962.

[14] M. Khilla, W. Gross, H. Schreiber, and D. Leucht, "Flexible Ka-Band LCAMP for in-orbit output power adjustable MPM," in *Proceedings of the 23rd AIAA International Communications Satellite Systems Conference (ICSSC '05)*, Rome, Italy, 2005.

[15] W. A. Sandrin, "The butler matrix transponder," *COMSAT Technical Review*, vol. 4, no. 2, pp. 319–345, 1974.

[16] S. Egami and M. Kawai, "An adaptive multiple beam system concept," *IEEE Journal on Selected Areas in Communications*, vol. 5, no. 4, pp. 630–636, 1987.

[17] M. Lisi, "An introduction to multiport power amplifiers," Microwave Engineering Europe, pp. 43–48, 1992.

[18] M. Aloisio, P. Angeletti, and M. Lisi, "Multiport amplifiers for satellite applications: historical perspective and future directions," in *Proceedings of the IEEE International Vacuum Electronics Conference (IVEC '09)*, pp. 201–202, Rome, Italy, April 2009.

[19] S. D'Addio, M. Aloisio, E. Colzi, and P. Angeletti, "Performance analysis of satellite payload output sections based on multiport amplifiers," in *Proceedings of the IEEE International Vacuum Electronics Conference (IVEC '09)*, pp. 207–208, Rome, Italy, April 2009.

[20] P. Angeletti and M. Lisi, "Multiport pwer amplifiers for flexible satellite antennas and payloads," *Microwave Journal*, vol. 53, no. 5, 2010.

[21] M. Aloisio, P. Angeletti, and S. D'Addio, "Statistical characterization of isolation performance of multiport amplifiers: a critical discussion," in *Proceedings of the IEEE International Vacuum Electronics Conference (IVEC '11)*, pp. 83–84, Bangalore, India, February 2011.

[22] M. Aloisio, P. Angeletti, and S. D'Addio, "Accurate modeling and analysis of isolation performance in multiport amplifiers," *Active and Passive Electronic Components*, vol. 2012, Article ID 738367, 4 pages, 2012.